Bažant, Z.P. (1994). "Recent advances in fracturemechanics, size effect and rate dependence of concrete: Implication for dams." Proc., *Int. Workshop on Dam Fracture and Damage*, held at Chambéry, France, March, A.A. Balkema, Rotterdam, 41–54.

PROCEEDINGS OF THE INTERNATIONAL WORKSHOP ON DAM FRACTURE AND DAMAGE / CHAMBERY / FRANCE / 16-18 MARCH 1994

Dam Fracture and Damage

Edited by

ERIC BOURDAROT

National Hydro Engineering Centre, Electricité de France, Savoie Technolac, France

JACKY MAZARS

Laboratoire de Mécanique et de Technologie, Ecole Normale Supérieure, Cachan, France

VICTOR SAOUMA

Civil Engineering Department, University of Colorado, Boulder, Colorado, USA

A.A. BALKEMA / ROTTERDAM / BROOKFIELD / 1994

Dam Fracture and Damage, Bourdarot, Mazars & Saouma (eds) © 1994 Balkema, Rotterdam, ISBN 90 5410 369 8

Recent advances in fracture mechanics, size effect and rate dependence of concrete: Implications for dams

Zdeněk P. Bažant
Department of Civil Engineering, Northwestern University, Evanston, Ill., USA

ABSTRACT: Recent researches have clearly demonstrated that the failure analysis of dams should be conducted according to the concepts of fracture mechanics. The present lecture presents an overview of some recent advances in this subject made at Northwestern University, and discusses their implications for dams. Attention is first focused on a comparison of the classical no-tension plastic analysis and fracture analysis. Although the no-tension analysis is normally on the safe side, this is not guaranteed to be always so, and counter examples of fracture analysis with cracks loaded by water pressure are given to show that fracture mechanics can yield a smaller resistance of the structure. Recent tests of the size effect in fracture of dam concrete are reviewed and the dependence of fracture, and especially of the size effect, on the rate of loading or loading duration is described. Generalization of the R-curve model for fracture and of the cohesive crack model (or the crack band model) for time-dependence are presented. Calculation of macro-fracture energy by particle simulation of microstructure is discussed and results indicating its dependence or microductility and on the coefficient of variation of microstrength are presented. The mathematical foundations of the basic scaling of plasticity and fracture mechanics are also reviewed. Various implications for the analysis on dams are discussed.

1 INTRODUCTION

Same as all concrete structures, the dams have been for a long time successfully designed using material failure criteria expressed in terms of stress and strain. The theoretical foundation for this approach to failure lies in the theory of plasticity. This classical theory is known to be applicable for materials that exhibit yielding, as manifested by a sufficiently prolonged yield plateau on the stress-strain diagram as well as on the measured load-deflection diagram of the structure. These characteristics, however, are not true for concrete. Except for very high hydrostatic pressures, concrete is a brittle (or more precisely quasibrittle) material which fails by fracture.

As is well known since the pioneering work of Griffith in 1921, fracture cannot be treated by stress criteria. The propagation of cracks must be determined on the basis of an energy criterion, which can equivalently be expressed either in terms of the stress intensity factor, when there is a stress singularity at a sharp crack tip, or in terms of stress-displacement relationship for the opening of a cohesive crack. Because of the quasibrittle nature of the material, the failure condition, aside from the fracture energy, also involves a strength limit, representing the strength of the material within the fracture process zone. The strength condition becomes irrelevant only when the fracture process zone is negligibly small compared to the length of the crack or to the cross section dimension of the structure. Concrete dams are usually sufficiently large to satisfy the condition, and in that case the strength limit can be omitted from the material fracture model, the fracture process zone can be considered to be a point, and thus linear elastic fracture mechanics (LEFM), in which the only material failure criterion is an energy criterion, can be applied.

The most important difference between fracture mechanics and plasticity is a difference in the size effect or the scaling law for structural failures. The size effect is expressed in terms of the nominal strength σ_N of the structure, which is defined as the maximum load (ultimate load) P_u divided by the characteristic dimension of the structure, D, and the structure thickness, b. More generally, P_u can be the parameter of a system of loads assumed to increase proportionally (thus the size effect for a static failure of a concrete dam can be defined only for geometrically similar dams for which both the vertical gravity loads and the hor-

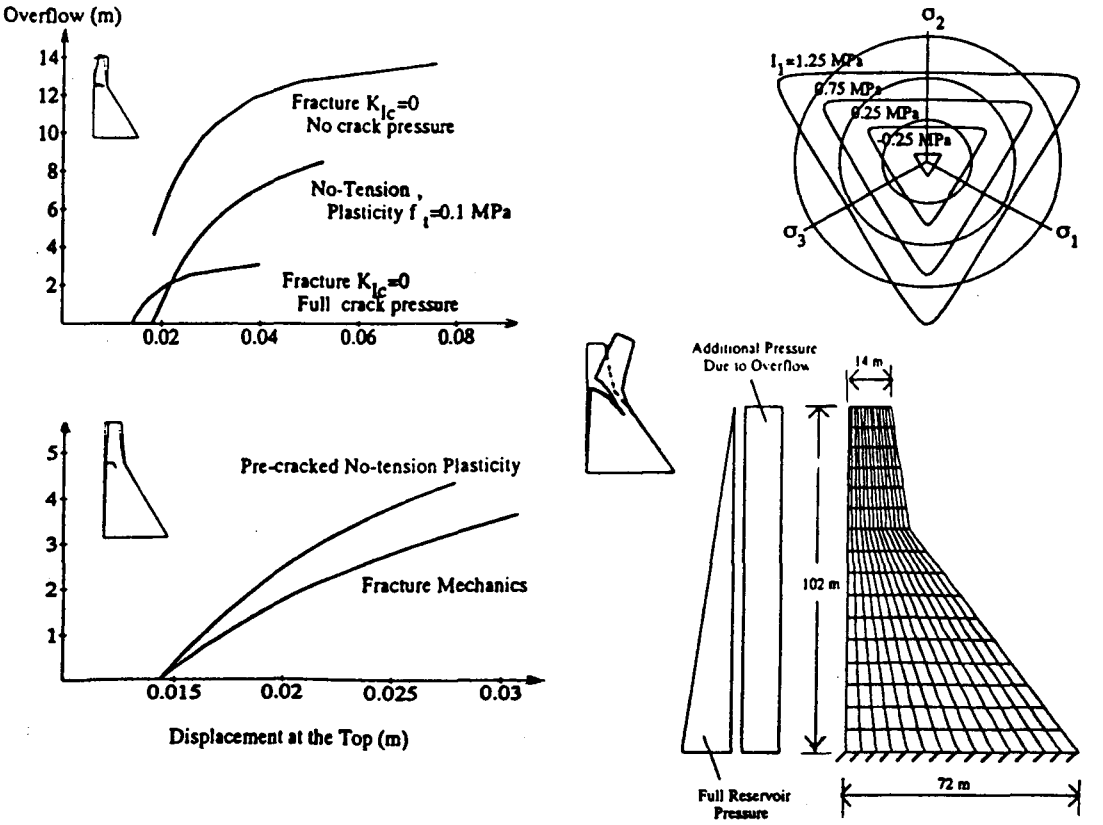

Figure 1: Left: Comparison of plots of overflow height of water versus horizontal displacement at the top of dam for no-tension plastic analysis of a precracked dam and for fracture analysis (water pressure, in the full value, is considered on the precracked portion of the cross section). Top Right: Ottosen's yield surface used. Lower Right: Dam analyzed, and mesh (after Gioia et al., 1992).

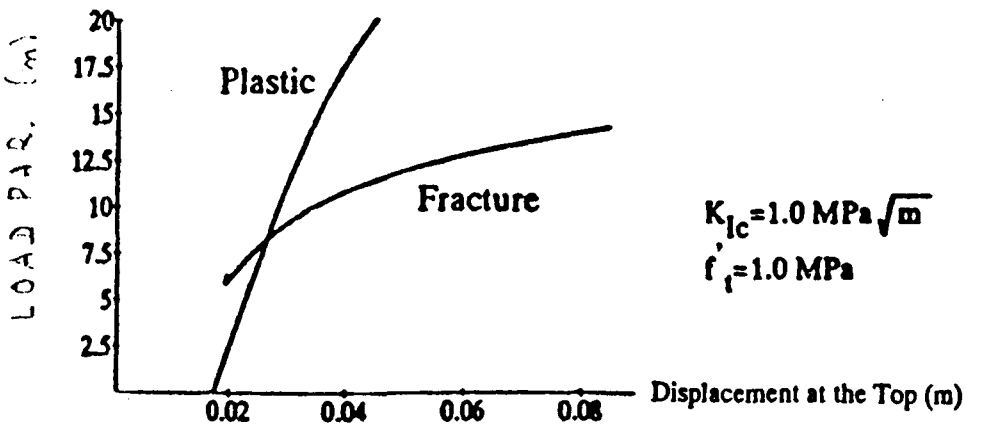

Figure 2: Comparison of the overflow-displacement curves for plastic and fracture analysis, using realistic values of tensile strength and fracture toughness (after Gioia et al., 1992).

izontal pressures from the reservoir are increased in proportion to one load parameter, P).

The size effect in quasibrittle failures of concrete structures, both reinforced and unreinforced, has recently become a subject of keen attention [1–7, 13–14] and has been reviewed in detail by an ACI Committee [8]. It has been established that the size effect caused by the energy release associated with fracture is a significant consideration in many design problems, including concrete dams [9–12]. It has been also shown that the duration of loading, and particularly the difference between a rapid loading such as an earthquake and a slow loading such as long-time volume changes of concrete or slow foundation settlements, is significant and needs to be taken into account in fracture analysis of dams [10, 12]. The purpose of this lecture is to review some recent advances relevant to fracture of dams which have been achieved at the speaker's home institution and present an overview of several new results and open problems.

2 Plastic analysis with zero tensile strength vs. fracture analysis

Because of the uncertainty in the value of the tensile strength of concrete, concrete dams have been designed under the assumption that the tensile strength of concrete is zero. This "no-tension" design has generally been believed to be on the safe side, which has however never been proven mathematically. Therefore, the question naturally arose whether fracture mechanics can give a smaller failure load than the classical no-tension design.

In an initial study of this question [9], idealized rectangular dam geometries which are amenable to the existing closed-form fracture mechanics solutions, have been considered. It was shown that when geometrically similar dam designs of various sizes are considered, there exists a certain critical size of a dam above which fracture mechanics gives a smaller failure load than the classical no-tension analysis. This question has been examined more systematically in [11], in which finite element solutions according to no-tension plasticity and according to fracture mechanics have been compared. The material constitutive model for no-tension plasticity has been considered as a special case of Ottosen's yield surface. Because a zero yield limit cannot be considered in plasticity, the calculations have been run for a negligibly small value of tensile yield strength of concrete, approximately 10 times smaller than a realistic value.

The differences between plasticity and fracture mechanics have been found to be most pronounced for the case when water penetrates into the crack and applies (uniformly distributed) pressure on concrete. Because, in plastic analysis, no actual crack can be considered in the model, the dam has been assumed to be precracked and loaded by the full reservoir pressure in the crack.

Some of the results from [11] are shown in Fig. 1. The load parameter is defined in terms of the height of the water overflow above the top of the dam, and a curved crack is considered. It is seen that in this case the fracture mechanics yields a lower resistance, for the same horizontal displacement at the top of the dam, than the plasticity solution with a negligible tensile strength and water pressure on a pre-existing crack. Fig. 2 shows a comparison of the plasticity solution and fracture solution when realistic values of the tensile strength f'_t (yield limit) and of K_{I_c} are considered.

From these examples quoted from [11] it transpires that the widely held assumption that the no-tension plastic design lies necessarily on the safe side is not always correct. The importance of taking the fracture mechanics approach appears to be greatest when there is water pressure on the crack surfaces.

3 Size effect and fracture characteristics of dam concrete

The basic material property of dam concrete which must be known for fracture analysis of a dam is the fracture energy G_f. Furthermore, as a second parameter, one needs to know also the characteristic length of the fracture process zone, c_f, which is related to the transitional size for the size effect. These properties have been studied extensively for concrete for almost two decades, however, until recently no specific information existed for dam concrete. Due to the large aggregate size as well as the relatively low strength and low cement content, different values of these basic properties must be expected for dam concretes.

Recently, systematic studies of the fracture properties of dam concretes have been conducted at the Swiss Federal Institute of Technology, Lausanne [15], University of Colorado, Boulder [14, 16], and (under a joint collaborative project) at Northwestern University and University of Wisconsin, Madison [12]. The last study also focused on another aspect which is important for dams, namely the effect of load duration or loading rate.

It was found [12] that the fracture behavior of dam concrete agrees quite well with the size effect law proposed by Bažant [1], and that testing of geometrically similar fracture specimens of various sizes makes it possible to determine the fracture energy and the effective length of the fracture process zone. Tests on dam concrete specimens (with 3 in. maximum aggregate size) were conducted on wedge-splitting (compact tension) fracture specimens of cross sections ranging from 30 cm to 182 cm, at loading rates leading to a maximum load within a second or up to several hours. It was shown [12] that the value of fracture energy of dam concrete is higher than for conven-

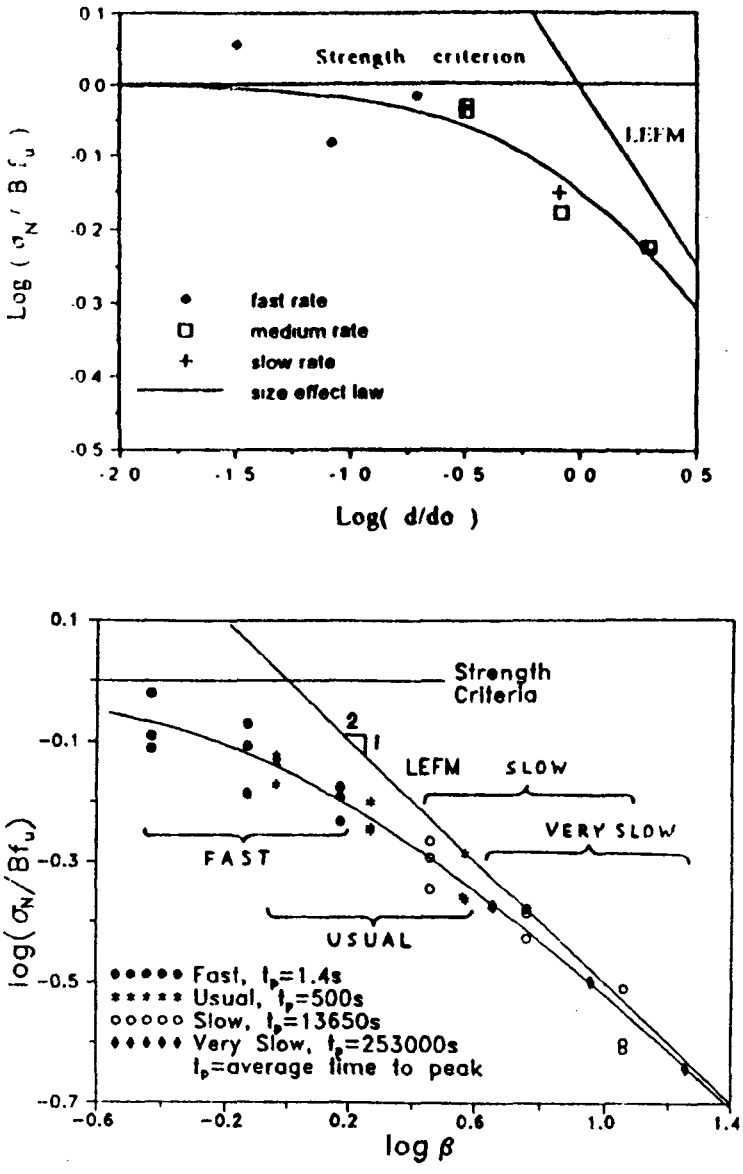

Figure 3: Size effect plots for various loading rates; top: for dam concrete (after He et al., 1992), bottom: for normal concretes (after Bažant and Gettu, 1992).

tional concretes with smaller aggregates. Also, the fracture energy value was found to increase with the loading rate.

A surprising result from this study of dam concrete [12] as well as a preceding similar study of normal concretes [17] was that, as the loading rate decreases, the fracture behavior becomes closer to linear elastic fracture mechanics; see Fig. 3 where the results for dam concrete [12] are shown on the left and the results for normal concrete [17] are shown on the right (the scatter of test results for dam concrete was larger, no doubt because of the greater difficulty to maintain precisely controlled environmental conditions and curing conditions for the very large specimens used for the dam concrete). This is manifested in the size effect plot of $\log \sigma_N$ versus $\log D$ by a shift of the test results to the right, that is, closer to LEFM.

This interesting property means that for long-time loading the concretes (both dam and normal concretes) are more brittle than for short-time loading. This property is not obtained for

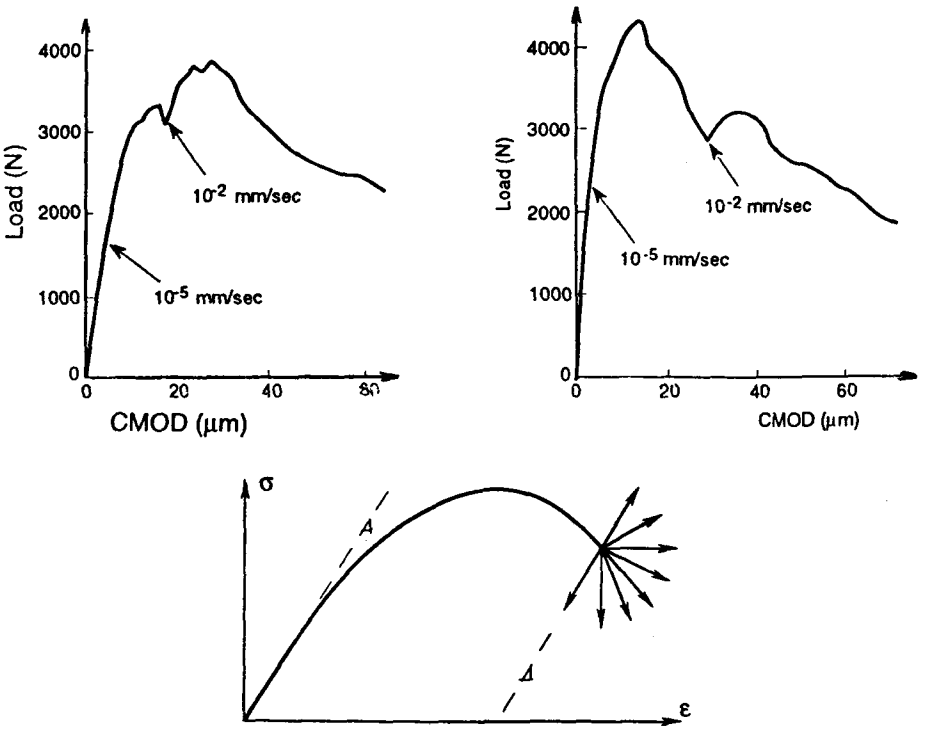

Figure 4: Reversal of softening to hardening caused by a 1,000-fold increase of the CMOD loading rate, for three-point-bend fracture specimens (after Bažant, Gu and Faber, 1993) (top); possible slopes after a sudden rate change.

rocks, which exhibit no creep [18]. So, the explanation obviously must be sought in the effect of creep in the fracture process zone as well as in the bulk of the specimen. Stress relaxation due to creep causes the fracture process zone to become smaller with time, that is, the length of the stress drop from the strength limit to zero ahead of the fracture tip becomes shorter with increasing load duration (for further detail see [12] and [17]).

4 New experimental and theoretical results on the rate and time effects in fracture

For the analysis of fracture of dams it is important to capture the effect of loading rate and load duration which came to light in [17] and [12]. In a dam, a crack may grow, due to volume changes or foundation movements, very slowly, over a period of many years. Then, when an earthquake strikes, the propagation of the crack may suddenly become very rapid.

Therefore, tests have recently been conducted at Northwestern University under sudden changes of the loading rate. Fig. 4 shows the measured response in the plot of load versus CMOD (crack mouth opening displacement) when the loading rate is increased 1,000× in the post-peak softening regime (the labels S, M, and L denote small, medium and large specimens). It is most interesting that, for such a large and sudden increase in the loading rate, the softening response can be reversed to hardening, followed by a second peak. From these tests it appears that by a sudden increase or decrease of the loading rate, all the directions of response shown in Fig. 4 are possible at a point in the softening regime. Thus, when an earthquake strikes, the initial response of a dam with an existing large crack might be hardening even though the previous crack has been growing in a softening regime.

Tests have also been conducted for a sudden decrease of the loading rate, and as a special case, for a sudden arrest of the CMOD displacement increase. The later case represents relaxation of the load at constant displacement. In concrete specimens, the relaxation was found to be very significant, and stronger in notched specimens than in unnotched specimens. This means that there is a significant contribution from increased creep in the fracture process zone, as compared to the linearly viscoelastic creep in the bulk of the structure [17]. In contrast with this behavior, rock fracture specimens exhibit no stress relaxation, obviously

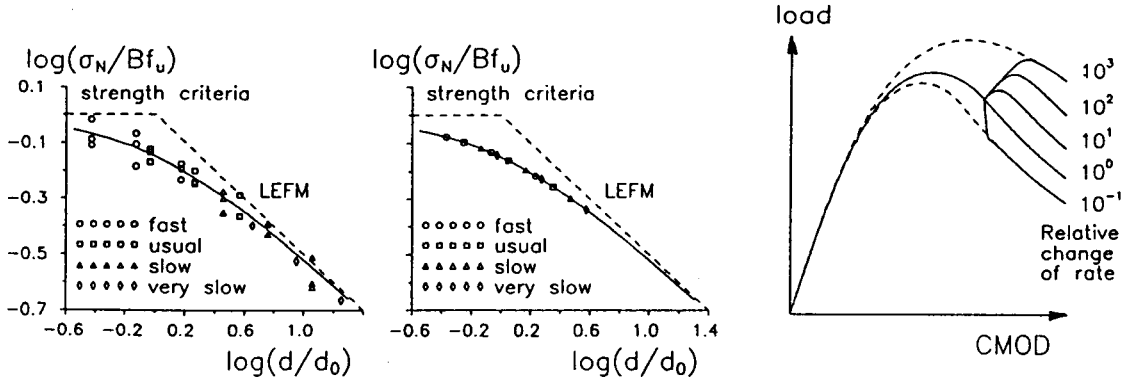

Figure 5: Top: Comparison of theory with experimental plots of peak load versus CMOD rates for different specimen sizes; middle: plot of nominal strength versus normalized size for different loading rates (left: theory, middle: experiment); right: calculated plot of load versus CMOD at sudden changes of the loading rate by factors ranging from 10^{-1} to 10^{3} (after Bažant and Jirásek, 1993).

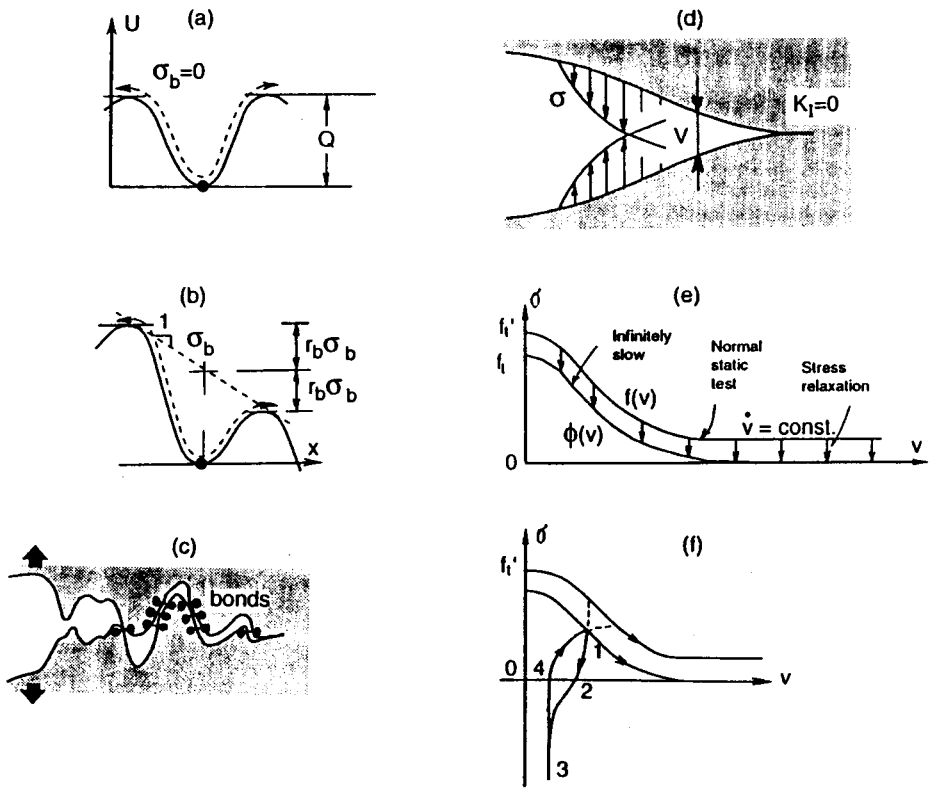

Figure 6: Activation energy concept (a, b), bond ruptures at fracture front (c), crack bridging stresses in the cohesive crack model (d), stress-displacement relation for the rate dependent model (e), and behavior at unloading and reloading (f) (after Bažant, 1993).

because rock does not creep [18].

The modeling of the rate effect in concrete fracture has been the subject of many studies [20–25]. For concrete, it is important to capture the nonlinear aspects of fracture caused by the finite size of the fracture process zone. The simplest way to describe them adequately is by the R-curve (resistance curve) approach.

The R-curve approach has recently been generalized to time-dependent behavior of concrete [26]. The basic relations of this generalized R-curve model are as follows:

$$\dot{a} = f(K, K_R) = \kappa \left(\frac{K}{K_R(\gamma)} \right)^n, \quad \gamma = \frac{c}{c_f} \qquad (1)$$

$$c_f = k\dot{a}^{1/m} \qquad (2)$$

$$u(t) = \int_{t_0}^{t} J(t, t') d\left\{ P(t') \bar{C}[a(t')] \right\} \qquad (3)$$

(Stielties integral). Here a = crack length, K = stress intensity factor caused by applied load, K_R = critical stress intensity factor required for crack propagation (the R-curve), which is a function of crack extension c from the end of the traction-free crack length; c_f, n, κ = constants; f = a function; c_f = effective length of the fracture process zone, considered as a function of the crack propagation rate $\dot{a}$; k, m = constants; u = deflection, t = current time, P = applied load, $\bar{C}$ = associated compliance for unit value of the elastic modulus, t' = time as an integration variable, t_0 = time of the first loading, and $J(t, t')$ = compliance function characterizing the linear viscoelastic aging creep of concrete (Eq. 3 is written for a unit thickness of the specimen).

By numerical integration of these equations [26] it has been demonstrated that all the available experimental results on the time effect of fracture of concrete can be described adequately. This is documented in Fig. 5, taken from [26], which shows (by the solid curves) the matching of the following types of tests: The plots of the peak load versus the CMOD rate for various sizes of geometrically similar three-point-bend fracture specimens, the size effect plots of normalized nominal strength σ_N versus the beam depth d (representing the characteristic dimension D), normalized by the transitional size d_0 of the size effect plot (the curve is the theoretically predicted size effect curve, which closely agrees with the size effect law [1], and the data points are the test data); and the calculated plots of load versus CMOD displacement for a sudden change of one loading rate to another (the dashed curves represent the response when the loading rate is constant from the beginning). It must be pointed out however that the present model was not able to provide as large a shift to the right in the peak load data for various loading rates as that revealed by the experimental results in the size effect plot (Fig. 5). For further details see [26].

5 Generalization of the cohesive (fictitious) crack model or crack band model for time dependence

A more realistic way of modeling the effect of time and loading rate on the fracture of concrete is a generalization of the cohesive (fictitious) crack model or the crack band model. Such a generalization has been presented in [27] and its numerical application with comparison of test results has been made in [28].

The rate effect in fracture stems from two sources. One source is obviously the creep, which occurs, in the case of concrete, in the entire volume of the structure. For most of the structural volume, one may consider the creep to be linear, but within the fracture process zone the creep is certain to be nonlinear. However, it is not clear whether a separate consideration must be given to the creep in the fracture process zone because time-dependent effects arising in the process zone may be included in a time dependent generalization of the fracture model itself.

The second source is the time dependence of the rupture of bonds. Although the classical fracture mechanics is a time-independent theory, the breakage of bonds, which is the origin of fracture, cannot happen instantly when the bond strength is exceeded, but occurs at a certain finite rate. This rate is governed by the statistics of the thermal vibrations of atoms or molecules. The law governing the rate of bond breakages responsible for the fracture can be derived in the following manner which is analogous to that used in material science models for creep or plastic flow (which also involves bond breakages) and is based on the same principle as the activation energy theory for the rate of chemical reactions [40–41].

The thermal vibrations of atoms or molecules, which have a typical frequency $\nu \approx 10^{13} s^{-1}$, are random and the frequency at which any specified energy level U is exceeded is given by the Maxwell-Boltzmann distribution, $f = k_b e^{-U/RT}$, in which T = absolute temperature, R = gas constant, k_b = constant = $\alpha\nu$, and α = entropy factor. The potential of the bond forces, U, which is schematically plotted in Fig. 6a as a function of the distance x from the equilibrium position, has a certain maximum, Q, near the equilibrium position. This maximum is called the activation energy Q. It must be overcome for the bond to rupture. Therefore, the rate of bond breakages is given by $f_b = k_b e^{-Q/RT}$.

Now, if stress σ_b is applied to the bond, the bond potential U is modified as schematically shown in Fig. 6b, with the result that the potential energy barriers for a particle (atom or molecule) escape to the right or left are changed to $U_2 = Q - r_b\sigma_b$ and $U_1 = Q + r_b\sigma_b$; here r_b represents the distance from the equilibrium position (minimum potential energy) to the maximum potential energy (the reason is that $r_b\sigma_b$ represents the work of the applied stress on displacement r_b). In

absence of applied stress σ_b, the potential energy barriers for movements to the left and right are equal, and so, even though the bonds rupture and the particles move, there is no net overall movement either to the right or to the left. However, when stress σ_b is applied, the frequency f_2 of the jumps over the potential energy barrier U_2 to the right exceeds the frequency f_1 of the jumps over the potential energy barrier U_1 to the left. Obviously, the rate of crack opening must be proportional to the difference of these two frequencies. Therefore, substituting the foregoing expressions for U_2 and U_1, we obtain

$$\begin{aligned} \dot{v} &= k_f(f_2 - f_1) \qquad (4) \\ &= k_b k_f \left[e^{-(Q-r_b\sigma_b)/RT} - e^{-(Q+r_b\sigma_b)/RT}\right] \\ &= 2k_b k_f \sinh\left(\frac{r_b\sigma_b}{RT}\right) e^{-Q/RT} \end{aligned}$$

It is now convenient to introduce the reference temperature T_0 and denote $C_0 = 2k_b k_f e^{-Q/RT_0} =$ constant. Furthermore, we need to relate the stress σ_b in the bonds that undergo fracturing to the overall crack bridging stress σ. To do this precisely, we would need to know the number of the resisting bonds, which is changing with the crack opening, as well as the deformation of crack surface which is influenced by the local stiffness of the microstructure at various parts of the crack surface. This aspect of modeling is obviously complicated, and a simplification must be introduced.

We will simply assume that σ_b is proportional to $\sigma - \phi(v)$ where $\phi(v)$ is a function that has the shape shown in Fig. 6f and is supposed to describe the stress-displacement relation $\sigma = \phi(v)$ of the cohesive crack model for an infinitely slow rate $\dot{v}$ of the crack opening. Thus we may set $(r_b/RT_0)\sigma_b = k_0[\sigma - \phi(v)]$, in which r_b, R, T_0 and k_0 are constants. With the aforementioned notations, Eq. (4) at reference temperature becomes

$$\dot{v} = C_0 \sinh\{k_0[\sigma - \phi(v)]\} \qquad \text{for} \quad T = T_0 \quad (5)$$

and Eq. (4) at any temperature T becomes

$$\dot{v} = C_0 \sinh\left(\frac{T_0}{T} k_0 [\sigma - \phi(v)]\right) \exp\left(\frac{Q}{RT_0} - \frac{Q}{RT}\right) \qquad (6)$$

Function $\phi(v)$ for an infinitely small rate of crack opening cannot be measured directly, and it is convenient to relate it somehow to the stress-displacement relation $\sigma = f(v)$ for fracture in the normal static tests in the laboratory. It seems that a simple but realistic assumption might be $\phi(v) = k_1 f(v)$, in which $\sigma = f(v)$ is the stress-displacement relation of the cohesive crack model (Fig. 6f) for the normal loading rate in a static test, that is, the loading rate that leads to the maximum load within about 5 min., and $k_1 =$ constant that is close to 1 but less than 1 (roughly $k_1 = 0.8$). Here it is assumed that the normal static test does not reduce the crack bridging stress to zero but terminates with a plateau $\sigma = \sigma_\infty$; σ_∞ is assumed to be a small positive constant roughly equal to $0.1 f_t'$ (f_t' = direct tensile strength).

The foregoing assumption might explain why in static tests the load-deflection diagrams have a curiously long tail and why normally the load is not seen to get reduced to zero even at very large deflections. This long tail might well be a consequence of the rate effect. To reduce the stress at very large v to 0 it is necessary to extend the test duration by several orders of magnitude, which causes stress relaxation, as indicated by the downward arrows in Fig. 6e. Fitting of experimental data is needed to determine whether such a simple assumption would be adequate. As for the behavior at unloading and reloading, it seems reasonable to delete the rate-dependence of fracture as long as the crack bridging stress is below $\phi(v)$.

The present model for rate-dependent crack opening either can be implemented directly in the form of a rate-dependent cohesive (fictitious) crack model, generalizing the model of Hillerborg et al., or it can be converted to a stress-strain relation for the crack band model or a nonlocal model for continuum damage (cracking) that leads to fracture. This is accomplished simply by setting $v = h\epsilon_f$ where ϵ_f is the fracturing strain in the stress-strain relation with softening and h is a characteristic length of the material which represents either the width of the crack band or a length over which the spatial averaging in the nonlocal continuum model is carried out.

The latter approach has been adopted by Wu and Bažant [28] in another paper. In that work, the rate-dependent fracture model is combined with a creep model for the material in the bulk of the specimen. The creep model is based on the solidification theory, with the creep of the cement constituent represented by the Kelvin chain model. It is shown in that paper that such a combined model for creep and fracture rate dependence compares favorably with the existing experimental data for various rates of loading and for various specimens sizes, and also reproduces the observed size effect reasonably well. It is also noted that inclusion of both creep in the bulk of specimen and the rate-dependence of the crack opening is important; if only one of these two phenomena is modeled, good agreement with the experimental data cannot be obtained. The creep in the bulk of the specimen has of course considerable effect on the stresses at the fracture tip. For slow loading or arrest of the increase of opening displacement, the creep causes significant stress relaxation around the fracture process zone, leading to its unloading.

Fig. 7, taken from [28] shows the numerical implementation of the cohesive crack model (after its transformation to an equivalent crack band model) in comparison with the experimental curves of load versus CMOD, for two very different times t_p to the peak load and for different speci-

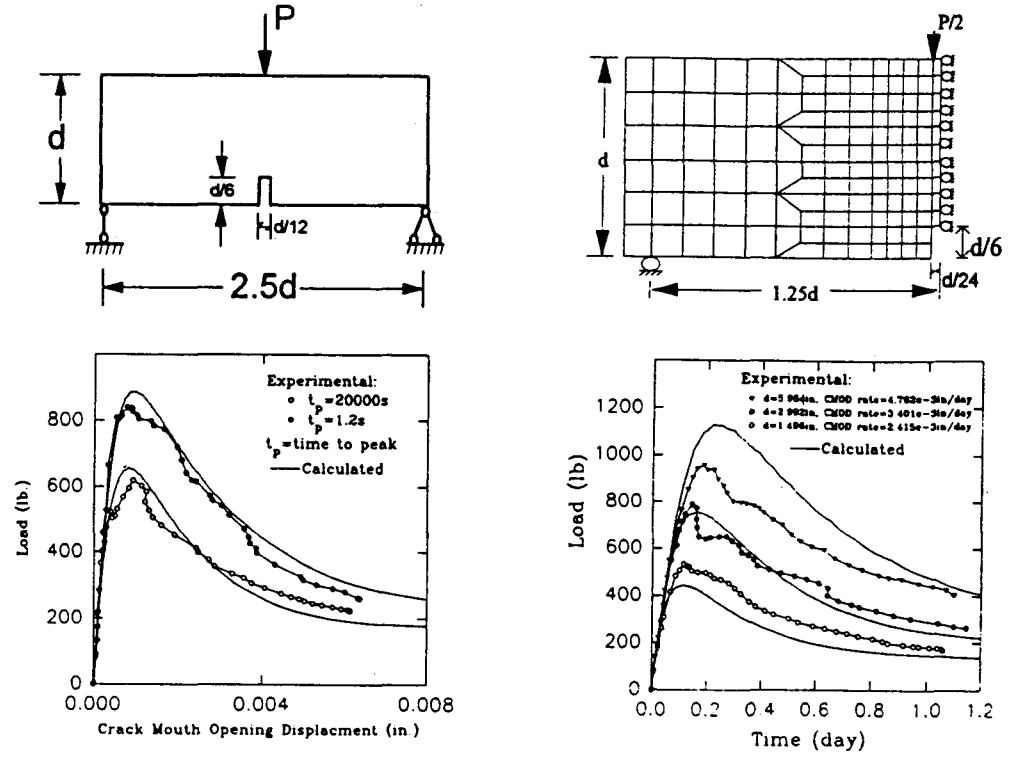

Figure 7: Fracture specimens analyzed, mesh used, and the response curves of load versus CMOD (left) or load versus time (right), measured and calculated (after Wu and Bažant, 1993).

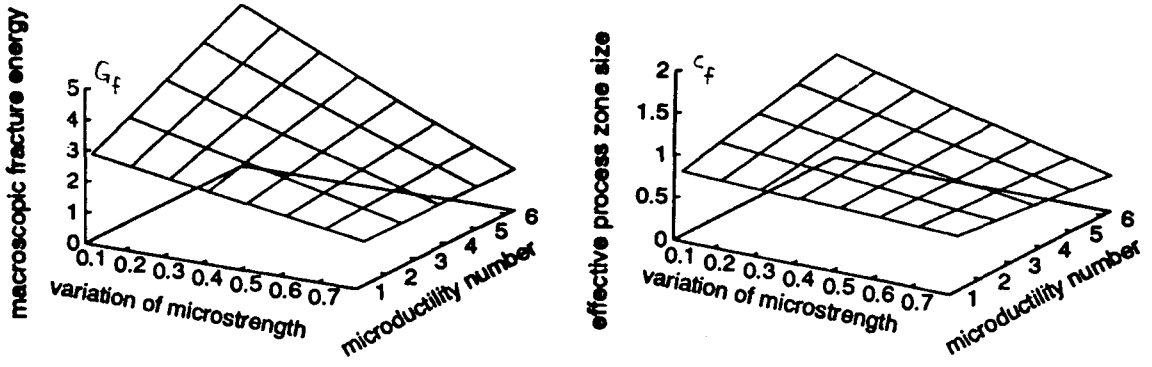

Figure 8: Mean macroscopic fracture energy G_f (left) and mean effective fracture process zone length c_f (right) as functions of microductility and coefficient of variation of microstrength (after Jirásek and Bažant, 1993).

men sizes. For further details see [28] (and more detail in a paper by Bažant and Wu to be completed by the time of the conference).

6 Determination of the macroscopic fracture properties of concrete by micromechanical analysis

The fact that the aggregate in dam concretes is relatively large, although not as large as it used to be in old dams, makes laboratory testing of fracture properties difficult because the specimens have to also be quite large. This is true even for the size effect method, which enables determining fracture properties from smaller specimens than other methods because it exploits the size effect law which extrapolates to very large sizes. For this reason, theoretical prediction of the macroscopic fracture energy on the basis of the known microscopic characteristics would be very helpful.

Studies of predicting macroscopic fracture properties for microscopic characteristics by means of the random particle model have been conducted at Northwestern University [39, 38]. The microstructure of concrete has been simulated by the random particle model in which interactions between adjacent large aggregate pieces are considered to occur through central forces only so that the microstructure can be described by a truss. The bars connecting the adjacent particles are assumed to behave elastically up to a certain strength limit and then to undergo linear softening to zero, characterized by a certain strain ϵ_f at which the stress is reduced to zero. The microstructure characteristics are defined by the elastic stiffnesses of the bars, the strength limit f_t', the value of ϵ_f, and the value of strain ϵ_p at the peak stress. A computer algorithm to generate randomly at two-dimensional system of particles according to the prescribed size distribution of the particles has been developed [39]. The size effect method [2] has been used, based on a simulation of three-point-bend fracture specimens of different sizes. From the maximum loads obtained in such simulations, the macroscopic fracture energy G_f and the effective length of the fracture process zone, c_f, have been determined according to the size effect method [8].

One important property that has been established from the studies conducted so far is the dependence of the mean G_f and mean c_f on the coefficient of variation of the microstrength f_t' (which has been generated as random, according to lognormal distribution) and on the microductility defined as the ratio ϵ_f/ϵ_p. This dependence, as obtained from a large number of numerical simulations according to the size effect method which ere smoothed by fitting with a bilinear function, is depicted by the surfaces in Fig. 8.

7 Concluding remarks

In conclusion of the preceding exposition, the following observations may be highlighted:

1. Failure of concrete dams ought to be analyzed by fracture mechanics. Although the current practice of using no-tension plasticity-type analysis is mostly on the safe side, a theoretical proof of the safety of this approach does not exist and counter examples are available, particularly for the case of cracks loaded by water pressure, in which the prediction of the no-tension design is not on the safe side.

2. An important consideration in fracture of dams is the size effect. Extrapolation must be made for relatively small laboratory specimens to structures of very large sizes, and this obviously necessitates a good model for the size effect on fracture. The size effect may also be exploited for determining the material fracture characteristics, particularly the fracture energy and the effective length of the fracture process zone (as well as the R-curve).

3. Fracture of concrete is highly time dependent. A faster loading generally gives a stiffer response. A sudden increase of the loading rate (which is important for the analysis of seismic events) causes a sudden stiffening of response, and may even reverse softening response to hardening response followed by a stress peak. The time dependence of fracture can be most easily modeled by a time-dependent generalization of the R-curve model, which represents an equivalent LEFM approach. More realistically, the cohesive (or fictitious) crack model as well as the crack band model, can be generalized to the time dependence, partially exploiting the activation energy theory for the rupture of bonds. These generalizations have provided a relatively good match of recent experimental data.

Acknowledgement.—Partial financial support under NSF Grant MSM-8815166 to Northwestern University if gratefully acknowledged. Additional financial support for the activation energy theory application has been received from the ACBM Center at Northwestern University.

APPENDIX: Basic scaling laws of plasticity and fracture mechanics

Because of the importance of size effect for the analysis of dams, an abbreviated account of a recent rigorous derivation of the elementary scaling laws of plasticity and linear elastic fracture mechanics, originally presented in [5], will now be given, for reader's convenience. For concrete

the size effect is more complicated, representing a transition between these elementary laws.

The size effect is defined by comparing geometrically similar structures of different sizes. We denote as Y the response quantity whose size dependence is to be determined—for example, the nominal strength (or nominal stress at failure), $Y = \sigma_N$, which is defined as $\sigma_N = c_N P_u/bD$ (for 2D) or $\sigma_N = c_N P_u/D^2$ (for 3D), in which P_u = maximum (ultimate) load, b = structure thickness in the case of two-dimensional similarity, D = characteristic dimension (or characteristic size), which can be chosen arbitrarily, and c_N = coefficient introduced for convenience.

Consider now theories in which there is no characteristic length. This means that the scaling ratio $\bar{Y}/Y$ of the corresponding responses $\bar{Y}$ and Y depends only on the size ratio $\lambda = \bar{D}/D$ of two different sizes $\bar{D}$ and D but is independent of the choice of the reference size D. Plasticity, elasticity with a strength limit, continuum damage mechanics (without nonlocal concepts), and also linear elastic fracture mechanics (LEFM) belong to this class of theories, and so do many other theories in physics. As is well known, the scaling law for all these theories is a power law. This can be shown by adapting an argument used in fluid mechanics (Barenblatt, 1979, 1987). Let the scaling law be $f(\lambda)$, that is $\bar{Y}/Y = f(\lambda)$, where f is an unknown function that we want to find. Considering another structure size $\tilde{D} = \mu D$ with the corresponding response $\tilde{Y}$, we have $\tilde{Y}/Y = f(\mu)$ Now, because there exists no characteristic size, the size $\bar{D}$ can alternatively be chosen as the reference size. In that case, $\tilde{Y}/\bar{Y} = f(\mu/\lambda)$.

Substituting here the preceeding equations, we obtain

$$f\left(\frac{\mu}{\lambda}\right) = \frac{f(\mu)}{f(\lambda)} \tag{7}$$

This is a functional equation from which the function $f(\lambda)$ can be solved. To this end, we differentiate Eq. (7) with respect to μ and then set $\mu = \lambda$; thus we get $f'(1)/\lambda = f'(\lambda)/f(\lambda)$, in which f' is the derivative of function f. The last equation is a differential equation for the unknown function f, which can be easily solved by separation of variables. With the notation $f'(1) = m$ = constant, the integral is $\ln f(\lambda) = m \ln \lambda + C$, and determining the integration constant C from the condition $C = \ln f(1) = 0$ for $\lambda = 1$, we have $f(1) = 1$. So we finally conclude that function f must be a power function,

$$f(\lambda) = \lambda^m \tag{8}$$

The power scaling law we obtained must hold for every physical system in which there is no characteristic dimension. This includes plasticity or elasticity with a strength limit. Further this includes LEFM.

Proving the converse, i.e., that there is no characteristic size if the scaling law is a power law, is obvious and trivial.

Consider now geometrically similar structures of different sizes. They are related by the affine transformation (affinity), which is the transformation of change of scale: $\bar{x}_i = \lambda x_i$, where x_i are the Cartesian coordinates for the reference structure of characteristic dimension (size) D, and $\bar{x}_i$ are the coordinates for a geometrically similar scaled structure and $\lambda = \bar{D}/D$ where $\bar{D}$ is the characteristic dimension of the scaled structure. The primes are used to label the quantities referring to the scaled structure. For the sake of brevity, we will denote $\partial/\partial x_i = \partial_i$, $\partial/\partial \bar{x}_i = \bar{\partial}_i$. From the chain rule of differentiation, $\partial_i = \lambda \bar{\partial}_i$, $\bar{\partial}_i = \lambda^{-1}\partial_i$.

For the reference structure of size D and the similar scaled structure of size $\bar{D}$, the field equations and the boundary conditions are

For D:

$$\partial_j \sigma_{ij} + f_i = 0 \tag{9}$$

$$\varepsilon_{ij} = (\partial_j u_i + \partial_i u_j)/2 \tag{10}$$

$$\sigma_{ij} n_j = p_i \quad \text{on } \Gamma_1 \tag{11}$$

$$u_i = U_i \quad \text{on } \Gamma_2 \tag{12}$$

For $\bar{D}$:

$$\bar{\partial}_j \bar{\sigma}_{ij} + \bar{f}_i = 0 \tag{13}$$

$$\bar{\varepsilon}_{ij} = (\bar{\partial}_j \bar{u}_i + \bar{\partial}_i \bar{u}_j)/2 \tag{14}$$

$$\bar{\sigma}_{ij} \bar{n}_j = \bar{p}_i \quad \text{on } \bar{\Gamma}_1 \tag{15}$$

$$\bar{u}_i = \bar{U}_i \quad \text{on } \bar{\Gamma}_2 \tag{16}$$

in which σ_{ij} and ε_{ij} are the stresses and strains in Cartesian coordinate x_i, u_i = displacements of material points, Γ_1 and Γ_2 are the portions of the boundary with prescribed surface tractions p_i and with prescribed displacements U_i; f_i = prescribed volume forces; and $n_j = \bar{n}_j$ = direction cosines of unit outward normals on the stress boundary.

From equation (9) we already know that the scaling law must be a power function. Let us now assume that the displacements are related by the scaling law

$$\bar{u}_i = \lambda^{m+1} u_i \tag{17}$$

where m is an unknown exponent. Substituting this into the differential equations and boundary conditions (13)-(16), we find $\bar{\varepsilon}_{ij} = \lambda^m(\partial_j u_i + \partial_i u_j)/2$. Then, assuming further that the stresses and strains obey the same scaling law, we get the following transformation rules:

$$\bar{\varepsilon}_{ij} = \varepsilon_{ij}\lambda^m, \quad \bar{\sigma}_{ij} = \sigma_{ij}\lambda^m, \quad \bar{\sigma}_N = \sigma_N \lambda^m$$

$$\bar{p}_i = p_i \lambda^m, \quad \bar{f}_i = f_i \lambda^{m-1}, \quad \bar{u}_i = u_i \lambda^{m+1} \tag{18}$$

These rules indicate how a solution for one size can be transformed to a solution for another size. However, the value of m is indeterminate. To determine it, we cannot ignore the constitutive law

and the failure condition. Next we consider in this regard two important special cases.

For an elastic-plastic constitutive law, the constitutive relation and the condition of no failure (either the yield condition or the condition of allowable stress) have the general form:

$$\sigma_{ij} = \mathcal{F}_{ij}(\varepsilon_{km}), \qquad \phi(\sigma_{ij}, \varepsilon_{ij}) < \sigma_0 \tag{19}$$

in which $\mathcal{F}_{ij}$ are tensor-valued functions or functionals of a tensorial argument, ϕ is a nonlinear scalar function of tensorial arguments, and σ_0 is the material yield limit or allowable stress limit. After transformation of scale, (19) takes the form $\bar{\sigma}_{ij} = \mathcal{F}_{ij}(\bar{\varepsilon}_{km})$, $\phi(\bar{\sigma}_{ij}, \bar{\varepsilon}_{ij}) < \sigma_0$. Since at least function ϕ (and possibly also function $\mathcal{F}$) is nonlinear (and nonhomogenous), this is possible only if $\bar{\sigma}_{ij} = \sigma_{ij}$ and $\bar{\varepsilon}_{km} = \varepsilon_{km}$, which means that $m = 0$. The transformation rules from Eqs. (17) and (18) then become

$$\begin{aligned} \bar{u}_i &= \lambda u_i, \quad \bar{\varepsilon}_{ij} = \varepsilon_{ij}, \quad \bar{\sigma}_{ij} = \sigma_{ij} \\ \bar{p}_i &= p_i, \quad \bar{f}_i = f_i/\lambda, \quad \bar{u}_i = u_i\lambda \end{aligned} \tag{20}$$

Also,

$$\bar{\sigma}_N = \sigma_N \tag{21}$$

that is, the nominal stress at failure does not depend on the structure size. We say in this case that there is no size effect. This is characteristic for all failure analyses according to elasticity with allowable stress limit, plasticity and classical continuum damage mechanics (as well as viscoelasticity and viscoplasticity, because time has no effect on this analysis).

In linear elastic fracture mechanics, the constitutive relation and the condition of no failure can be written as

$$\sigma_{ij} = D_{ijkm}\varepsilon_{km}, \qquad J < G_f \tag{22}$$

in which D_{ijkm} is the fourth-order tensor of elastic constants, G_f is the fracture energy (considered as a material property), and J is the J-integral;

$$J = \oint \left(\frac{1}{2}\sigma_{ij}\varepsilon_{ij}\mathrm{d}y - \sigma_{ij}n_j\partial_1 u_i \mathrm{d}s \right) \tag{23}$$

Using the transformation rules in (17)–(18), we find that the J-integral transforms as

$$\begin{aligned} \bar{J} &= \oint \left[\frac{1}{2}(\lambda^m\sigma_{ij})(\lambda^m\varepsilon_{ij})\lambda \mathrm{d}y \right. \\ &\qquad \left. -\lambda^m\sigma_{ij}n_j\lambda^{-1}\partial_1(\lambda^{m+1}u_i)\lambda \mathrm{d}s \right] \\ &= \lambda^{2m+1}\oint \left(\frac{1}{2}\sigma_{ij}\varepsilon_{ij}dy - \sigma_{ij}n_j\partial_1 u_i ds \right) \\ &= \lambda^{2m+1}J \end{aligned} \tag{24}$$

Since both $\bar{J}$ and J must satisfy the same inequality, that is, $\bar{J} < G_f$ and $J < G_f$ in all cases, it is obviously necessary and sufficient that $2m + 1 = 0$, that is,

$$m = -1/2 \tag{25}$$

Thus, according to (14) and (15), the transformation laws for linear elastic fracture mechanics are

$$\bar{u}_i = u_i\sqrt{\lambda}, \quad \bar{\varepsilon}_{ij} = \varepsilon_{ij}/\sqrt{\lambda}, \quad \bar{\sigma}_{ij} = \sigma_{ij}/\sqrt{\lambda}$$

$$\bar{p}_i = p_i/\sqrt{\lambda}, \quad \bar{f}_i = f_i\lambda^{-3/2}, \quad \bar{U}_i = U_i\sqrt{\lambda} \tag{26}$$

$$\bar{\sigma}_N = \frac{\sigma_N}{\sqrt{\lambda}} \tag{27}$$

where $\lambda = D/\bar{D}$. So the nominal stress at failure depends on the structure size $D, \sigma_N \sim 1/\sqrt{D}$ or

$$\log \sigma_N = \text{constant} - \frac{1}{2}\log D. \tag{28}$$

So, in the plot of $\log \sigma_N$ versus $\log D$, the linear elastic fracture mechanics failures are represented by a straight line of slope $-\frac{1}{2}$, while all stress- or strain-based failure criteria correspond to a horizontal line.

From the foregoing derivation, it is clear that fracture mechanics leads to a different scaling than plasticity. This is important to note with regard to dams.

In an alternative manner, which is shorter but abstract and less convincing, the size effect can also be determined [5] by dimensional analysis, on the basis of Buckingham's Π theorem of dimensional analysis [29–37].

References

1. Bažant, Z. P. (1984). "Size effect in blunt fracture: Concrete, rock, metal." *J. of Engng. Mechanics*, ASCE, 110, 518–535.
2. Bažant, Z. P., and Pfeiffer, P. A. (1987). "Determination of fracture energy from size effect and brittleness number." *ACI Materials Jour.*, 84, 463–480.
3. "Size effect in concrete structures," Preprints of JCI (Japan Concrete Institute) Int. Workshop held in Sendai, Japan, Oct. 31–Nov. 2, 1993, organized by H. Mihashi, Tohoku University.
4. Bažant, Z.P. (1993). "Size effect in tensile and compressive quasibrittle failures." *ibid*, 141–160.
5. Bažant, Z.P. (1993). "Scaling Laws in Mechanics of Failure." *J. of Engrg. Mech.*, ASCE, 119(9), 1828–1844.

6. Carpinteri, A. (1984). "Scale effects in fracture of plain and reinforced concrete structures", in *Fracture Mechanics of Concrete: Structural Application and Numerical Calculation*, ed. by G.C. Sih and A. DiTommaso, Martinus Nijhoff Publ., The Hague, 95–140.

7. Carpinteri, A. (1986). *Mechanical damage and crack growth in concrete*, Martinus Nijhoff Publ., Dordrecht—Boston (chapter 8).

8. ACI Committee 446, Fracture Mechanics (Z.P. Bažant, Chairman). (1992) "Fracture mechanics of concrete: Concepts, models and determination of material properties." ACI Special Publication, 1R-91, American Concrete Institute, Detroit, MI., 1991 (146 pp.); reprinted in *Fracture Mechanics of Concrete Structures*, ed., Z.P. Bažant, Elsevier, London, 1–140.

9. Bažant, Z. P. (1990). "A critical appraisal of 'no-tension' dam design: A fracture mechanics viewpoint." *Dam Engineering* 1(4), 237–247.

10. Bažant, Z.P., He S., Plesha, M.E., and Rowlands, R.E. (1991) "Rate and size effect in concrete fracture: Implications for dams." (Proc., Int. Conf. on Dam Fracture, Denver, Colorado, September), ed. by V. Saouma, R. Dungar, and D. Morris, University of Colorado, 413–425.

11. Gioia, G., Bažant, Z.P., and Pohl, B. (1992), "Is no-tension dam design always safe?", *Dam Engineering* 3(1), 23–34.

12. He, S., Plesha, M.E., Rowlands, R.E., and Bažant, Z.P. (1992) "Fracture energy tests of dam concrete with rate and size effects." *Dam Engineering* 3(2), 139–159.

13. Brühwiler, E. (1991). "Fracture of mass concrete under simulated seismic action." *Dam Engineering*, 1(3).

14. Saouma, V.E., Brühwiler, E., and Boggs, H.L. (1990). "A review of fracture mechanics applied to concrete dams." *Dam Engineering*, 1(1).

15. Brühwiler, E., and Wittmann, F.H. (1988). "The wedge splitting test, a method of performing stable fracture mechanics tests." Proceedings *Int. Conf. on Fracture and Damage of Concrete and Rock*, Vienna.

16. Saouma, V.E., Broz, J.J., Brühwiler, E., and Boggs, H.L. (1991). "Effect of aggregate and specimen size on fracture properties of dam concrete." *J. of Engineering Materials*, ASCE, 3(3).

17. Bažant, Z.P., and Gettu, R. (1992). "Rate effects and load relaxation: Static fracture of concrete." *ACI Materials Journal*, 89(5), 456–468.

18. Bažant, Z.P., Bai, S.-P., and Gettu, R. (1993). "Fracture of rock: Effect of loading rate." *Engineering Fracture Mechanics*, 45(3), 393–398.

19. Bažant, Z.P., Gu, W.-H., and Faber, K.T. (1993). "Softening reversal and other effects of a change in loading rate on fracture behavior." Report, Northwestern University, 1993; also ACI *Materials Journal*, in press.

20. Liu, Z.-G., Swartz, S.E., Hu, K.K., and Kan, Y.-C. (1989). "Time-dependent response and fracture of plain concrete beams." *Fracture of concrete and Rock: Recent Development*, eds. S.P. Shah, S.E. Swartz and B. Barr, Elsevier Applied Science, London, 577–586.

21. Mindess, S. (1985). "Rate of loading effects on the fracture of cementitious materials." *Application of Fracture Mechanics to Cementitious Composites*, ed. S.P. Shah, Martinus Nijhoff Publ., Dordrecht, pp. 617–638.

22. Reinhardt, H.W. (1985). "Tensile fracture of concrete at high rates of loading." *Application of Fracture Mechanics to Cementitious Composites*, ed. S.P. Shah, Martinus Nijhoff Publ., Dordrecht, pp. 559–592.

23. Reinhardt, H.W. (1986). "Strain rate effects on the tensile strength of concrete as predicted by thermodynamic and fracture mechanics models." *Cement-Based Composites: Strain Rate Effects on Fracture*, eds. S. Mindess and S.P. Shah, 1–14.

24. Wittmann, F.H. (1985). "Influence of time on crack formation and failure of concrete." *Application of fracture mechanics to cementitious composites*, ed. S.P. Shah, Martinus Nijhoff Publ., Dordrecht, pp. 593–616.

25. Ross, C.A., and Kuennen, S.T. (1989). "Fracture of concrete at high strain-rates." *Fracture of Concrete and Rock: Recent Developments*, eds. S.P. Shah, S.E. Swartz and B. Barr, Elsevier Applied Science, London, UK, pp. 152–161.

26. Bažant, Z.P. and Jirásek, M. (1993). "R-curve modeling of rate and size effects in quasibrittle fracture." *Int. Journal of Fracture*, 62, 355–373.

27. Bažant, Z.P. (1993). "Current status and advances in the theory of creep and interaction with fracture." Proc., *5th International RILEM Symposium (ConCreep 5)*, held at U.P.C., Barcelona, September, ed. by Z.P. Bažant and I. Carol, E & FN Spon, London, 291–307.

28. Wu, Z.-S., and Bažant, Z.P. (1993). "Finite element modeling of rate effect in concrete fracture with influence of creep." Proc., *5th International RILEM Symposium (ConCreep 5)*, held at U.P.C., Barcelona, September, ed. by Z.P. Bažant and I. Carol, E & FN Spon, London,

29. Buckingham, E. (1914)." On physically linear systems; illustrations of the use of dimensional equations", *Physical Review* Ser.2. Vol.IV, No.4, 345–376.

30. Buckingham, E. (1915). "Model experiments and the form of empirical equations". *Trans. ASME* 37, 263–296 (also *Phys. Rev.* 4, 345–376).

31. Bridgman. P.W. (1922). *Dimensional analysis*, Yale University Press, New Haven.

32. Porter, A.W. (1933). *The method of dimensions*, Methuen.

33. Giles, R.V. (1962). *Theory and problems of fluid mechanics and hydraulics*, McGraw Hill, New York (chapter 5).

34. Streeter, V.L., and Wylie, E.B. (1975). *Fluid mechanics* (6th ed.), McGraw Hill, New York (chapter 4).

35. Barenblatt, G.I. (1979). *Similarity, self-similarity, and intermediate asymptotics*, Consultants Bureau, New York and London.

36. Barenblatt, G.I. (1987). *Dimensional analysis*, Gordon and Breach, New York.

37. Iyanaga, S., and Kawada, Y., Editors (1980). *Encyclopedic dictionary of mathematics*, MIT Press, Cambridge, Sec. 120 (pp. 412–413).

38. Jirásek, M. and Bažant, Z.P. (1993). "Macroscopic fracture characteristics of random particle systems." Report, Dept. of Civil Engineering, Northwestern University; submitted to *Int. J. of Fracture.*

39. Bažant, Z. P., et al. (1990). "Random particle model for fracture of aggregate or fiber composites." ASCE *J. of Engng. Mech.*, 116(8) 1686–1705.

40. Cottrell, A.H. (1964). The mechanical properties of matter. J. Wiley, New York.

41. Hertzberg, R.W. (1983). Deformation and fracture mechanics of engineering materials, 2nd ed., J. Wiley, New York.